2006

# Brittle Compressive Failure of Ice: Proportional Straining vs Proportional Loading

E. M. Schulson
*Dartmouth College*

D. Iliescu
*Dartmouth College*

## Dartmouth Digital Commons Citation

Schulson, E. M. and Iliescu, D., "Brittle Compressive Failure of Ice: Proportional Straining vs Proportional Loading" (2006). *Open Dartmouth: Published works by Dartmouth faculty*. 2570.
https://digitalcommons.dartmouth.edu/facoa/2570

# Brittle compressive failure of ice: proportional straining vs proportional loading

E.M. SCHULSON, D. ILIESCU

*Thayer School of Engineering, Dartmouth College, Hanover, New Hampshire 03755-8000, USA*
*E-mail: erland.schulson@dartmouth.edu*

**ABSTRACT. Proportional straining experiments have been performed on columnar-grained S2 fresh-water ice biaxially compressed across the columns at –10°C at a strain rate of $(4.5 \pm 1.5) \times 10^{-3}$ s$^{-1}$. The results are compared with those obtained earlier (Iliescu and Schulson, 2004) from the same kind of material deformed to terminal failure under the same conditions, but through proportional loading. The exercise shows that the biaxial strength is practically independent of the path taken, at least under low confinement where Coulombic shear faulting limits terminal failure. First-year sea ice is expected to exhibit the same behavior.**

## 1. INTRODUCTION

The biaxial compressive stress state that develops within the arctic sea-ice cover during winter (Richter-Menge and Elder, 1998; Richter-Menge and others, 2002) could arise through either proportional loading or proportional straining, or through a combination of loading paths. Along the first, the less compressive or minor principal stress, $\sigma_2$, is proportional to the more compressive or major principal stress, $\sigma_1$, through a constant of proportionality, $R$, that defines the loading path in principal stress space, i.e. $R = \sigma_2/\sigma_1$. Along the second path, the minor principal strain, $\varepsilon_2$, is proportional to the major principal strain, $\varepsilon_1$, through a constant of proportionality, $\chi$, that defines the straining path in principal strain space. Were the ice to behave in a purely elastic manner and were the elastic properties to be isotropic within the loading plane (as they are for S2 ice, described below), the two paths would be related through Hooke's law for isotropic materials, namely $\chi = (R - \nu)/(1 - R\nu)$ where $\nu$ is Poisson's ratio. However, the behavior of interest in relation to the structural integrity of a floating ice sheet is not purely elastic: an abundance of cracks and faults at many scales populates the winter cover (Kwok, 2001; Marsan and others, 2004; Schulson, 2004) and contributes to its deformation; and viscous processes may operate as well, as evident from creep buckling. The question thus arises: does the biaxial compressive strength depend upon the path taken to terminal failure?

We present here the results of a series of experiments designed to address this issue. We limit our attention to brittle behavior (i.e. to the kind that ice exhibits when rapidly compressed) and focus specifically on the regime of lower confinement where failure occurs through the nucleation, growth and interaction of secondary cracks that ultimately lead to the development of one or more Coulombic shear faults (Schulson and others, 1999; Renshaw and Schulson, 2001; Schulson and others, in press).

## 2. EXPERIMENTAL PROCEDURE

In recent work (Schulson and others, in press) we presented the complete failure envelope for first-year S2 sea ice, as measured through $R$-type loading of test specimens harvested from the winter cover of 2003 on the Beaufort Sea. While performing that work, we consumed all of the material we had harvested. Thus, we could not perform $\chi$ tests on the same ice. However, upon comparing the sea-ice envelope with one we had previously generated through $R$-loading (Iliescu and Schulson, 2004) of fresh-water ice of similar growth texture and grain-size, we found that the strength and the failure modes of the two materials were practically indistinguishable under the conditions examined (–10°C, major principal strain rate of $0.5\text{–}1.0 \times 10^{-2}$ s$^{-1}$). Therefore, we performed a series of $\chi$ tests using S2 fresh-water ice, and then compared these results to those obtained earlier from the $R$ tests on this material.

We produced the ice by unidirectionally freezing Hanover tap water, following the procedure described by Iliescu and Schulson (2004). The material consisted of columnar-shaped grains elongated in the growth direction, of average column diameter $6 \pm 2$ mm. Thin-section analysis (Iliescu and Schulson 2004) revealed that the crystallographic *c* axes of the individual grains were confined more or less to the horizontal plane of the parent ice sheet, but randomly oriented within this plane, in keeping with the microstructure of S2 ice (Michel and Ramseier, 1971). From the parent sheet, we prepared plate-shaped specimens of dimensions 152 mm × 152 mm × 25 mm. The long axis of each grain was perpendicular to the larger faces of the specimens.

We performed the experiments at –10°C. The specimens were deformed by compressing in two orthogonal directions across the columns, using the same multiaxial loading system used during the earlier work. Across-column displacements were measured using two calibrated extensometers mounted on J-shaped canes that were attached to solid brass loading platens. (A more desirable procedure would have been to attach displacement gauges directly to the ice.) The major strain rate was $\dot{\varepsilon}_1 = (4.5 \pm 1.5) \times 10^{-3}$ s$^{-1}$. We set the minor strain rate to be a fixed proportion of the major rate. Over the course of the experiments, we varied the straining path over the range $-1 < \chi < 0$, where the strain ratio was determined from the total strains.

We calculated the elastic component of strain using Hooke's law (taking Young's modulus to be $E = 10$ GPa and Poisson's ratio to be $\nu = 0.3$ (Gammon and others, 1983)), and then subtracted this component from the total strain to obtain the inelastic strain. The ratio of the inelastic strain components at terminal failure was greater than the ratio of the total components: generally $\chi_{\text{inelastic}} \sim 1.5\chi_{\text{total}}$. We attribute this difference mainly to the development of cracks preferentially aligned along the direction of shortening and

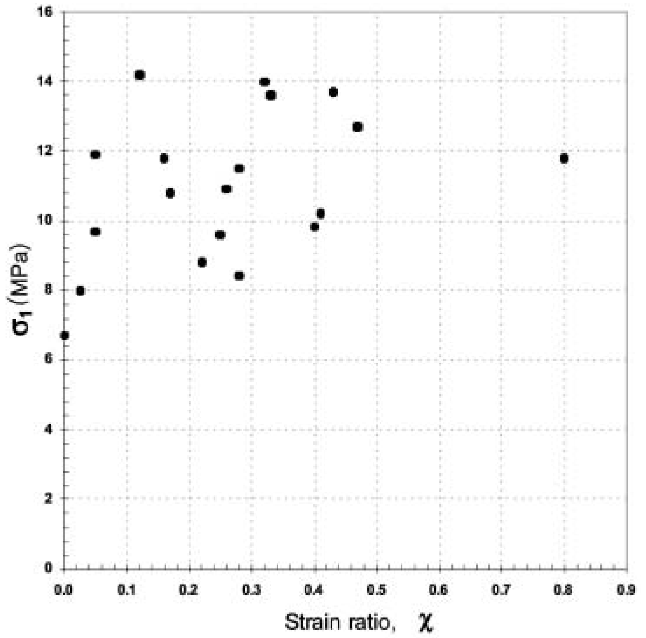

**Fig. 1.** Graph of terminal failure stress vs applied strain ratio for S2 columnar-grained fresh-water ice of 6 ± 2 mm column diameter deformed through proportional straining across the columns at –10°C at a strain rate (along the direction of shortening) of $4.5 \pm 1.5\,\mathrm{s}^{-1}$.

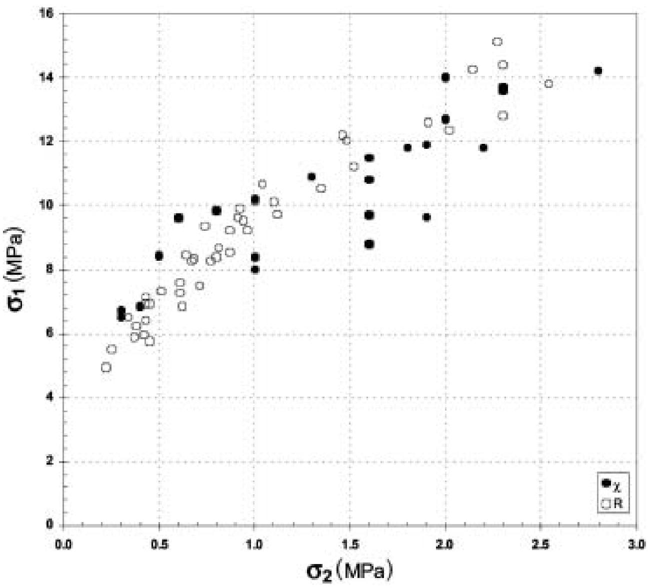

**Fig. 2.** Graph of terminal failure stress vs confining stress for the material described in Figure 1, showing data obtained through proportional straining tests ($\chi$; closed symbols) and data obtained by Iliescu and Schulson (2004) through proportional loading (*R*; open symbols). (Note that Figure 1 contains four fewer points than this figure because lateral strains were not recorded in four tests.)

parallel to the columnar-shaped grains and thus to the attendant increase in lateral displacement. Viscous flow may also have contributed to the difference, although to a degree we did not assess. In analyzing the results, however, we simply used the total strain, because we measured it.

## 3. RESULTS AND DISCUSSION

The ice exhibited brittle behavior over all $\chi$ paths; that is, the applied stress, after increasing more or less linearly with increasing strain, dropped suddenly as terminal failure set in. Failure occurred once the ice had shortened by 0.15–0.3%, through the development of a Coulombic fault inclined at $\theta = 27 \pm 3°$ to the direction of shortening, just as it did under proportional loading. Several small load drops (~10% of load) usually preceded terminal failure and corresponded to the initiation of secondary cracks, beginning once the load reached about one-half the terminal limit. The secondary cracks were oriented along the direction of shortening and parallel to the columns. Occasionally, a larger drop (~20–30%) preceded terminal failure, after which the load increased but to a level lower than the pre-drop level. We took the terminal failure stress to be the highest value of $\sigma_1$ registered during each experiment, and this we termed the strength of the ice. (This definition of strength is to be distinguished from the so-called differential strength, a term used in rock mechanics and defined as the difference between the maximum and minimum principal stress at failure.)

The strength showed essentially negligible correlation ($r^2 = 0.12$) with the applied strain ratio (Fig. 1). Instead, it correlated quite well ($r^2 = 0.82$) with the confining stress at terminal failure (Fig. 2). This behavior is not surprising. The theory of brittle compressive failure under low confinement (Horii and Nemat-Nasser, 1985; Ashby and Hallam, 1986; Renshaw and Schulson, 2001) dictates that failure evolves through a combination of frictional sliding across deformation-induced cracks plus initiation and propagation of secondary cracks along the direction of shortening, implying that strength depends sensitively upon confining stress. Generally, the evolution of deformation damage is somewhat variable from specimen to specimen, so the resulting lateral displacement is variable as well. Thus, when deformed along a prescribed $\chi$ path, some specimens develop relatively few cracks and so experience little induced lateral confining stress; others develop a greater crack density and thus experience greater induced confining stress. As a result, the brittle compressive strength is expected to vary rather widely for a given value of $\chi$, as observed from Figure 1.

Figure 2 shows that within the scatter in the data, and with the exception of 3 outlying points (out of 23), the strength measured under proportional straining, at least under the range of low confinement considered in these studies, appears to be practically indistinguishable from the strength previously measured for the same kind of ice deformed under proportional loading at the same temperature and strain rate (Iliescu and Schulson, 2004). In other words, if there is an effect of the path taken to terminal failure, it is a small one.

Our finding, of course, applies specifically to the behavior of S2 fresh-water ice. However, we expect that it also applies to first-year sea ice that possesses the same growth texture. This we base on the fact that the failure envelopes and the failure modes of the two materials, provided they have a similar grain-size, are essentially indistinguishable, at least at –10°C, as already mentioned.

## 4. CONCLUSION

From experiments on the brittle failure of columnar-grained S2 fresh-water ice compressed across the columns at –10°C at a strain rate of $(4.5 \pm 1.5) \times 10^{-3}\,\mathrm{s}^{-1}$, we conclude that the biaxial strength of the material along paths of proportional straining is practically indistinguishable from the biaxial strength along paths of proportional loading, at least under low confinement where terminal failure along either path is limited by Coulombic shear faulting.

## ACKNOWLEDGEMENTS

We acknowledge W.D. Hibler, III, for valuable discussions. The work was supported by US National Science Foundation grant No. OPP-0328605.

## REFERENCES

Ashby, M.F. and S.D. Hallam. 1986. The failure of brittle solids containing small cracks under compressive stress states. *Acta Metall. Mater.,* **34**(3), 497–510.

Gammon, P.H., H. Kiefte, M.J. Clouter and W.W. Denner. 1983. Elastic constants of artificial and natural ice samples by Brillouin spectroscopy. *J. Glaciol.,* **29**(103), 433–460.

Horii, H. and S. Nemat-Nasser. 1985. Compression-induced microcrack growth in brittle solids: axial splitting and shear failure. *J. Geophys. Res.,* **90**(B4), 3105–3125.

Iliescu, D. and E.M. Schulson. 2004. The brittle compressive failure of fresh-water columnar ice loaded biaxially. *Acta Mater.,* **52**(20), 5723–5735.

Kwok, R. 2001. Deformation of the Arctic Ocean sea ice cover between November 1996 and April 1997: a survey. *In* Dempsey, J.P., H.T. Shen and L.H. Shapiro, *eds. Scaling laws in ice mechanics and ice dynamics*. Dordrecht, etc., Kluwer Academic Publishers, 315–323.

Marsan, D., H. Stern, R. Lindsay and J. Weiss. 2004. Scale dependence and localization of the deformation of Arctic sea ice. *Phys. Rev. Lett.,* **93**(17), 178501. (10.1103/PhysRevLett.a3.178501.)

Michel, B. and R.O. Ramseier. 1971. Classification of river and lake ice. *Can. Geotech. J.,* **8**(1), 36–45.

Renshaw, C.E. and E.M. Schulson. 2001. Universal behaviour in compressive failure of brittle materials. *Nature,* **412**(6850), 897–900.

Richter-Menge, J.A. and B.C. Elder. 1998. Characteristics of pack ice stress in the Alaskan Beaufort Sea. *J. Geophys. Res.,* **103**(C10), 21,817–21,829.

Richter-Menge, J.A., S.L. McNutt, J.E. Overland and R. Kwok. 2002. Relating Arctic pack ice stress and deformation under winter conditions. *J. Geophys. Res.,* **107**(C10), 8040. (10.1029/2000JC000477.)

Schulson, E.M. 2004. Compressive shear faults within arctic sea ice: fracture on scales large and small. *J. Geophys. Res.,* **109**(C7), C07016. (10.1029/2003JC002108.)

Schulson, E.M., D. Iliescu and C.E. Renshaw. 1999. On the initiation of shear faults during brittle compressive failure: a new mechanism. *J. Geophys. Res.,* **104**(B1), 695–705.

Schulson, E.M., A. Fortt, D. Iliescu and C.E. Renshaw. In press. Brittle failure envelope of first-year Arctic sea ice. *J. Geophys. Res.*

*MS received 10 January 2006 and accepted in revised form 13 March 2006*